Underwater Explosion Response of Sandwich Structures with Compliant Cores

Brian Hayman

1 Introduction

Sandwich structures using polymer foams as the core material have been utilised in naval ships since the 1970s. Such foams give a stiffness in the thickness direction that is appreciably lower than many other potential core materials. Some foams have the potential to absorb large amounts of energy during crushing or other forms of deformation. Thus, foam-cored sandwich may offer possibilities for reducing the effect of shock and blast loadings, i.e. for shock mitigation. However, the task of establishing the real potential of these materials for shock mitigation, especially with regard to underwater explosions (UNDEX) presents several challenges, some of which will be presented here.

2 Brief History of Foam-Cored Sandwich in Naval Ships

According to Hellbratt and Gullberg [22] and Gullberg and Olsson [18], Swedish research and development work on foam-cored GRP sandwich structures for naval ships began in the mid to late 1960s in a collaboration between the Swedish Defence Materiel Administration and the Royal Institute of Technology (KTH). The core materials considered were structural rigid PVC foams. Shock testing showed that this kind of construction performed better than single-skin glass fibre reinforced plastics (GFRP) and traditional wooden construction. The semi-scale 24 m mine countermeasure vessel (MCMV) *Viksten*, which used this concept, was delivered in 1974. After further development and testing, including UNDEX shock

B. Hayman (✉)
Technical University of Denmark, Kongens Lyngby, Denmark
e-mail: bhayman@mek.dtu.dk

S. Gopalakrishnan and Y. Rajapakse (eds.), *Blast Mitigation Strategies in Marine Composite and Sandwich Structures*, Springer Transactions in Civil and Environmental Engineering, https://doi.org/10.1007/978-981-10-7170-6_2

testing of two full-scale test sections, seven *Landsort* Class MCMVs were built for the Swedish Navy, and four more for the Singapore Navy, at the naval shipyard in Karlskrona. The first vessel was delivered in 1984; extensive details are provided by Sjögren et al. [41]. The *Landsort* Class MCMVs were followed by the smaller *Styrsö* Class (four vessels) and by a series of 50 m *Standard Flex* multipurpose vessels for the Danish Navy.

Hellbratt and Gullberg [22] and Gullberg and Olsson [18] referred also to several other Swedish ships, including two 50 m coastguard vessels delivered in the late 1970s and two high-performance surface effect ships (SES) delivered in 1987–1988 for passenger ferry service. A 30 m, 40 km experimental SES with stealth properties, *Smyge*, was due for delivery in 1990–1991; further details were provided by Hellbratt and Gullberg [21] and Olsson and Lönnö [35]. This vessel was designed for dynamic loadings including slamming, but not UNDEX.

In spite of the favourable experience gained in Scandinavia, few other countries adopted the sandwich concept for MCMVs or other naval ships. The main exception was the Australian *Bay Class* inshore minehunter [19, 36, 37].

In the UK, the first major application of fibre composites in a naval ship was the Royal Navy's prototype MCMV *HMS Wilton*, which was commissioned in 1973. Before that, numerous small patrol boats and landing craft had been built in composites, but it was recognised in the late 1960s that the non-magnetic properties of composites could be exploited in MCMV applications, replacing wood as the main structural material. HMS *Wilton* was followed by the *Hunt* Class MCMVs. These were all of stiffened (framed) single-skin GFRP laminate construction. According to Henton [23], Dixon et al. [12] and Chalmers et al. [5], foam-cored sandwich construction had been evaluated but found to have inadequate fire and shock performance. However, the 'sandwich' concept tested appears to have been more like a cellular construction, with internal GFRP webs connecting the inner and outer face sheets [12]; with such internal stiffening the advantage of through-thickness compliance is lost. The discussion of the papers by Sjögren et al. and Chalmers et al. (RINA [38], Vol III) provides an insight into the different perceptions of fire and shock threats, and the different levels of achievement with sandwich hull structures, in the UK and Sweden at that time. However, in the UK, sandwich construction was later used in the superstructure of the *Sandown* Class minehunters [13]. In Italy, a thick GFRP monocoque design, the *Lerici* Class [43], was adopted for MCMVs and later developed into the *Osprey* Class MCMVs for the US Navy [44]. In 1984, the US Navy had previously ordered a lightweight SES concept with 'glass-reinforced plastic structure based on proven Swedish technology' [1, 2] but this programme was cancelled in 1986.

In Norway, a series of high-speed passenger ferries were built in the 1980s, based on the SES concept with PVC foam-cored GFRP composite construction. Meanwhile, the Royal Norwegian Navy (RNON) identified a need to replace its wooden *Sauda* Class MCMVs. Following the success of the *Landsort* MCMV design, together with the Swedish and Norwegian lightweight concepts for passenger ferries using SES technology, RNON began studying the feasibility of using foam-cored sandwich in a relatively lightweight, moderately high-speed concept

that would suit the long Norwegian coastline. The concept was finally adopted and seven vessels were built in the 1990s. These were followed by the development of the *Skjold* Class fast attack craft, but these did not have an UNDEX requirement.

A comprehensive overview of the application of reinforced polymer composites in naval vessels up to about year 2000 is provided by Mouritz et al. [32].

3 Norwegian MCMV Development Programme

In the late 1980s, Det Norske Veritas (DNV, now DNV GL) participated in the series of projects to establish the feasibility of building the Royal Norwegian Navy's new fleet of MCMVs as surface effect ships in foam-cored GFRP sandwich. In a preliminary study, the author attempted to simulate the response of foam-cored sandwich panels to underwater explosions and investigate whether their resistance to such events would be adequate for use in the MCMV hulls. In contrast to steel ship structures, little published work was found at that time on UNDEX response of composite ship structures, and no detailed information was found regarding the response of foam-cored sandwich panels.

The initial studies concluded that the response could be considered in two main phases: the initial, 'very early time' response as the incident shock wave strikes the panel and induces deformations with strain rates of the order $10^3\ s^{-1}$ in the thickness direction of the sandwich composite, and the later 'global' response of the panel as a whole involving bending and transverse shear deformations. In the first phase, the maximum pressure of the incident pulse appeared to be the dominant factor, while in the later phase the total impulse imparted to the panel was more important. The simulations for the initial phase indicated maximum compressive and tensile stresses in the thickness direction that were far in excess of the published static compressive and tensile strengths of available foam cores; thus it was decided that studies of the strain rate dependence of the foam core would be needed. The simulations of the global panel response involved a large degree of uncertainty; it was concluded, in particular, that the modelling of fluid–structure interaction (FSI) must take proper account of cavitation in the water. On the basis of these preliminary studies, it was clear that future simulations must be accompanied by realistic UNDEX tests on full-scale panels, both to validate the simulations and to demonstrate the performance of the final choice of layup.

3.1 UNDEX Tests

The Norwegian UNDEX tests were performed on air-backed panels representing the anticipated bottom panels of the MCMVs. The face sheets were GFRP laminates and the cores were of cross-linked, closed cell Divinycell PVC foam. Based on some early considerations, the panel size (the exposed area between supports)

was chosen as 1500 mm × 1600 mm. The tests were performed jointly by DNV and RNON at the Haakonsvern Naval Base.

More than 50 UNDEX tests were performed. It was necessary to investigate solutions that would satisfy a serviceability type criterion (the event should not cause significant permanent damage, and the ship should be able to withstand repeated shocks at this level) as well as a more extreme survivability criterion. Thus, many of the tests were performed at levels low enough to avoid noticeable damage, so the materials could be modelled as elastic, while others were at levels expected to cause significant, permanent damage. The tests were performed on full-scale panels with realistic charges and (far field) standoffs, and were to a large extent concerned with finding the most severe shocks that could be sustained while retaining full structural integrity, as well as providing detailed data for validating simulation methods. This contrasts with the emphasis that is often laid on maximising energy absorption and providing structural protection, with the sandwich possibly being treated as a sacrificial appendage that must be replaced when damaged.

The three test series involved in all six panels.

Series 1 Two nominally identical, instrumented panels were subjected to 14 UNDEX tests. The face sheets were of GFRP combimat, a combination of E-glass woven roving and chopped strand mat (CSM), with an iso-polyester matrix. The core was Divinycell H200 cross-linked PVC foam. The panels were placed vertically, with their centres 5 m below the water surface. The charges were placed at the same depth, directly in front of the panel centre. A range of charges and standoffs was used, the smallest standoff being 16 m. Only the primary shock wave was expected to affect the critical part of the panel response, so the measurements were mainly confined to this phase of the response. Several tests were performed at relatively low to medium shock levels in order to test repeatability and gather data for comparison with simulations before the shock level was increased to establish the shock capacity. Based on these tests, the simulation methods were modified and attempts were made to determine the layups that would be required to meet the design criteria for the MCMV bottom panels.

Series 2 Two panels, with thicker laminates and denser cores, and two different core thicknesses, were subjected to 16 UNDEX tests. The primary objective was to demonstrate the required shock resistance for application in the MCMVs. However, a few low-medium level shocks were also applied. The tests were mainly similar to those of Series 1, but a few were performed with the panel just below the water surface, to check the effects of surface cut-off (due to the negative reflected wave from the water surface). After the low-medium level shock tests, 100 kg TNT charges were used at decreasing standoffs until failure was observed.

Series 3 Two further panels, with modified face sheet materials compared to Series 1 and 2, were subjected to a total of 21 UNDEX tests. One panel was similar to those in Series 1, but with somewhat thicker face sheets containing a finer woven fabric and only a minimum of CSM. The other panel had thicker face sheets and a

heavier core material. This series included some tests similar to those of the earlier series, but also a large number of tests giving a range of angles of attack and panel and charge depths.

The panels were bolted to one face of an air-filled, welded steel box. This face of the box was open, but fitted with steel flanges 150 mm wide at each edge. The outermost 150 mm of each edge of the test panel were clamped between steel strips and these flanges, leaving the desired area 1500 mm × 1600 mm unsupported between the flanges. The box and TNT charges were held in position by wire ropes, a concrete block on the sea bed and a series of buoys. Figure 1 shows the arrangement for Series 1; minor modifications were made in the subsequent series.

All panels were fitted with strain gauges on the inside and outside face laminates and inside the core. The core gauges were placed so as to record strains in the thickness direction and at ±45°; the latter type of core gauges were intended to measure out-of-plane shear strains, which can be critical for panel performance (though this was not performed successfully in the first test series). A pressure transducer was suspended approximately 920 mm in front of the panel centre.

The strain gauges and pressure transducer were connected to twin-channel transient recorders, which were the only data capture devices available at that time that were fast enough to record the signals. In Series 1 and 2, a total of eight data channels were recorded. In Series 3, an extended arrangement allowed recording of up to 12 additional channels. Recording by the transient recorders was triggered by the incoming pressure signal. Sampling intervals in the range 1–10 μs were used, with the shortest intervals for the pressure and through-thickness strain signals; in

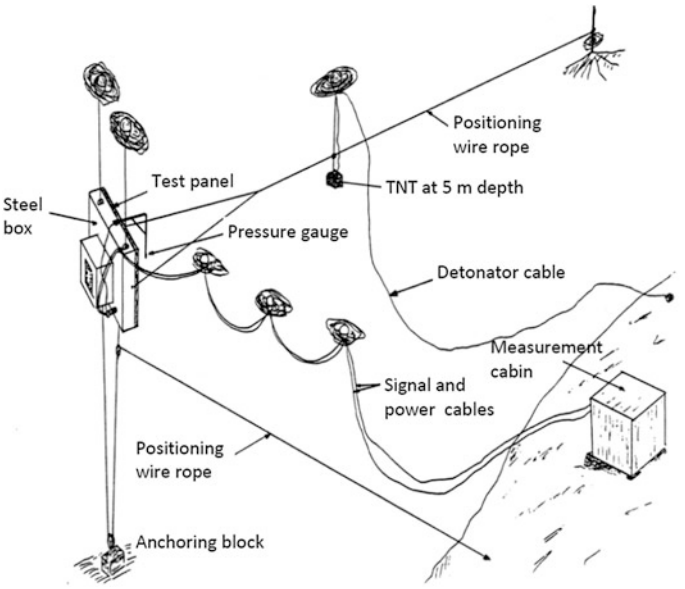

Fig. 1 Test arrangement for first Norwegian UNDEX test series

most cases, the duration recorded was 4096 samples. Paper plots were generated and the data were stored on 3½ inch diskettes in a now obsolete Hewlett Packard format. However, almost all of the test data have recently been retrieved and transferred to modern storage media.

3.2 UNDEX Simulations

At the time of the Norwegian studies, modelling of response and resistance to underwater explosions for composite vessels seems to have been considered unrealistic, although a considerable body of knowledge had been built up concerning the UNDEX response of steel ship hulls during and after the Second World War. Thus, investigation of the suitability of different composite concepts was mainly confined to experimental testing. Furthermore, as mentioned by Mouritz et al. [33], such investigations were often based on simple pass/fail tests and little was done during testing to measure the response or examine closely the failure mechanisms.

The first *published* reports on modelling of UNDEX response of foam-cored sandwich composite structures, to the author's knowledge, appeared in the early 1990s, after the Norwegian studies were completed. Moyer et al. [34] reported on a series of UNDEX tests performed in Sweden on instrumented 2 m × 2 m full-scale ship hull panels mounted on a rebuilt submarine hull section. They also described simulations of these tests using a modified version of DYNA3D based on a doubly asymptotic approximation (DAA) approach [16] and including the effects of surface cut-off (when the wave reflected from the water surface cancels or modifies the tail of the incoming wave) and associated cavitation. The simulations were confined to early times, before fluid flow effects become significant. Good agreement with the corresponding test results was demonstrated. This and later simulations are discussed in Sect. 4.

In parallel with the Norwegian UNDEX tests, analyses were carried out to simulate the panel responses and to perform parametric studies investigating the effects of changing the sandwich layup and the panel dimensions. The simulations were carried out using the finite element program FENRIS, which was coupled to the SESAM suite. FENRIS was an advanced FE program for nonlinear static and dynamic structural analysis; it was used partly for its geometrically nonlinear analysis capabilities and partly because it had good facilities for analysis of transient dynamic response. Composite materials were not implemented; the face sheets were modelled using a combination of bar and membrane elements that approximated the orthotropic elastic properties of the laminates. Attention was confined to the response to the primary shock wave as it was clear that the most severe part of the panel response would occur before the arrival of the subsequent bubble pulses.

The loading was defined with the aid of the empirical approximate formula for the pressure history due to a TNT charge W kg at standoff R m

$$p_i(t) = p_0 e^{-\alpha t}, \tag{1}$$

where

$$p_0 = 52.4\left(W^{1/3}/R\right)^{1.13} \tag{2}$$

and

$$\alpha = 1000/\left(0.0925 W^{0.26} R^{0.22}\right) \tag{3}$$

Here, p_i and p_0 are pressures in MPa, t is time in seconds and α (the reciprocal of the decay time constant) is in s^{-1}.

In the initial studies, various ways of modelling the fluid–structure interaction, as the shock wave struck the panel, were attempted. It was noted that, *for a thin plate*, the early time response could be adequately modelled using the acoustic equation for the resultant pressure on the plate surface [25, 42]:

$$p(t) = 2p_i(t) - \rho c v(t), \tag{4}$$

where ρ and c are the density and acoustic speed for the water and $v(t)$ is the velocity of the plate surface. In combination with the equation of motion for the plate, this predicts that, almost as soon as the plate is set in motion, the pressure just in front of the plate becomes negative, implying that cavitation will occur. Attempts were made to apply this directly in the FE analysis of a sandwich panel by using dashpot elements to represent the second term on the right-hand side of the above equation, and then assuming cavitation occurs as soon as the pressure at the panel surface drops to zero. The plate was then allowed to vibrate freely without any connection to the water. The effect of nonzero cavitation pressures was also investigated; the main effect of this is to move the cavitation site a short distance away from the plate surface. When compared with the first test results, this approach was found to give responses with timescales up to the maximum plate deflection that were much too short. If, instead, cavitation was suppressed and an added mass was assumed in accordance with accepted practice for vibrating, air-backed plates, the simulation gave far too slow a response. It appeared that a response with the correct timescale could only be obtained if it was assumed that a layer of water with thickness of the order 20 cm moved with the plate. The simulations were then performed in two stages: a first phase in which Eq. 1 is applied to the panel with dashpot elements representing the acoustic term, and a second stage in which the dashpots were removed and an extra mass corresponding to 20 cm of water was added to the panel surface.

A possible explanation for this was later given by Hayman [20]. An analysis was presented in which the one-dimensional, linear wave propagation equation was applied to the incoming pressure pulse, its transmission through the face sheet on the water side (assumed to be thin but with mass) and into the core, then its

reflection from the air side face sheet, and finally the wave transmitted back through the wet face sheet and into the water, combining with the tail of the initial incoming wave and the first reflection. This showed that the pressure in the water would drop to zero at *two* sites, one close to the panel surface and one about 10–20 cm away from it. Thus, a body of water of thickness 10–20 cm would be separated from both the panel and the remaining water. Study of the particle velocity of this body of water indicated that it would catch up with the panel as soon as the panel started to slow down as a result of its boundary constraints. This work demonstrated that the through-the-thickness compliance of the foam core has a fundamental influence on the fluid–structure interaction, the incidence of cavitation and the resulting panel response. This analysis is summarised in Sect. 3.3.

In the same analysis, equations were provided for calculating the thickness of the water layer and the 'kick-off' velocity given to this and the panel itself. Approximate, explicit expressions for these quantities were also provided. Under the assumption that the thickness of water moving with the panel remained constant, the subsequent panel motion and stress histories could be easily calculated.

The general approach, in which the occurrence of cavitation was calculated based on one-dimensional wave theory, was subsequently used by Mäkinen in a more detailed analysis in which movement of the cavitation boundaries was also taken into account (see Sect. 4.1). More recent investigations elsewhere have taken cavitation into account with varying degrees of accuracy.

3.3 Simulations: Summary of Analysis by Hayman [20]

The analysis presented by Hayman [20] contained some minor errors in the presented equations. A shortened, corrected version is provided here

3.3.1 Governing Equations

The free field pressure due to the incident pressure wave as it approaches the panel is assumed to be of the form

$$p_i(x,t) = p_0 e^{\alpha(x-ct)/c} \tag{5}$$

in which t is the time, measured from the instant at which the wave arrives at the panel surface, x is the distance from the panel surface (taken as positive into the panel), and c, p_0 and α are as defined previously. It is assumed that all distances x considered in the analysis are small compared with the standoff, so that the wave can be considered plane, and its amplitude can be considered constant as it travels. It is further assumed that the shock wave can be described by linear wave theory. This gives a uniform pressure at the panel surface given by Eq. 1.

On reaching the panel surface, the wave is partly transmitted into the panel and partly reflected. If the outer (water-exposed) skin laminate is thin compared to the sandwich core, it can be approximated by an infinitely thin sheet having a mass per unit area m_f. Then, it is only necessary to consider a transmitted wave in the core and a reflected wave in the water. The pressures at the skin laminate associated with the transmitted wave in the core and the reflected wave in the water are denoted by $p_{c1}(t)$ and $p_{r1}(t)$, respectively. These, and waves generated subsequently, are illustrated in Fig. 2.

The equation of motion for the skin laminate can be written as

$$p_i(t) + p_{r1}(t) - p_{c1}(t) = m_f \dot{v}_1(t) \tag{6}$$

in which $v_1(t)$ is the velocity of the laminate in the positive x direction. The particle velocities at the panel surface for the incident, reflected, and transmitted waves, u_i, u_{r1} and u_{c1}, respectively, are given by

$$u_i = \frac{p_i(t)}{\rho c}, u_{r1} = -\frac{p_{r1}(t)}{\rho c}, u_{c1} = \frac{p_{c1}(t)}{\rho' c'}, \tag{7}$$

where c' and ρ' are the acoustic speed and density for the foam core. The equations for this phase of the response are completed by the compatibility relationships between velocities:

$$u_i(t) + u_{r1}(t) = u_{c1}(t) = v_1(t) \tag{8}$$

When combined with the initial condition $v_1(t) = 0$, Eqs. 5–8 give

$$p_{c1}(t) = \rho' c' v_1(t) = A\left(e^{-\alpha t} - e^{-\beta t}\right) \tag{9}$$

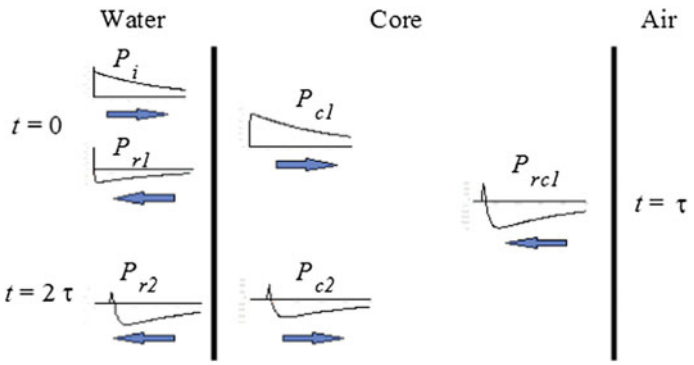

Fig. 2 Waves passing through water and sandwich core. From Hayman [20]

and

$$p_{r1}(t) = p_i(t) - \rho c v_1(t) = B_1 e^{-\alpha t} + B_2 e^{-\beta t}, \tag{10}$$

where

$$A = \frac{2\gamma p_0}{\beta - \alpha}; \quad B_2 = \frac{2(\beta - \gamma) p_0}{(\beta - \alpha)}; \quad B_1 = p_0 - B_2 \tag{11}$$

and

$$\beta = (\rho c + \rho' c')/m_f; \quad \gamma = \rho' c'/m_f \tag{12}$$

Full expressions for the transmitted and reflected waves $p_{c1}(t\text{-}x/c)$ and $p_{r1}(t\text{+}x/c)$ as functions of x and t are obtained if t is replaced by $(t\text{-}x/c)$ in Eq. 9 and by $(t\text{+}x/c)$ in Eq. 10, respectively.

The transmitted wave is assumed to pass through the core without attenuation, i.e. damping in the core is neglected. The wave reaches the rear (air side) laminate after a time interval τ, where

$$\tau = h_c/c' \tag{13}$$

in which h_c is the core thickness. What happens when the wave reaches the rear laminate (Fig. 2) can be described in a similar way to that used for the front laminate. However, there is a time-shift τ, and the wave that is transmitted into the air behind the panel can be neglected. For simplicity, the rear laminate will be assumed identical to the front laminate.

Then, it can be shown that the velocity of the rear laminate, w_1, is given by

$$w_1(t) = C_1 e^{-\alpha t'} + C_2 e^{-\beta t'} + C_3 e^{-\gamma t'} \tag{14}$$

and the wave that is reflected back through the core, p_{rc1}, is given by

$$p_{rc1}(t) = D_1 e^{-\alpha t'} + D_2 e^{-\beta t'} + D_3 e^{-\gamma t'} \tag{15}$$

in which

$$C_1 = \frac{4\gamma p_0}{(\beta - \alpha)(\gamma - \alpha) m_f}; \quad C_2 = \frac{4\gamma p_0}{(\beta - \alpha)(\beta - \gamma) m_f}; \quad C_3 = -(C_1 + C_2) \tag{16}$$

$$D_1 = \frac{-2\gamma(\alpha + \gamma) p_0}{(\beta - \alpha)(\gamma - \alpha)}; \quad D_2 = \frac{-2\gamma(\beta + \gamma) p_0}{(\beta - \alpha)(\beta - \gamma)}; \quad D_3 = -(D_1 + D_2) \tag{17}$$

and

$$t' = t - \tau \tag{18}$$

When the wave that has been reflected back through the core reaches the front skin laminate after a further time interval τ, a similar event occurs to that described previously. A wave $p_{r2}(x, t)$ is transmitted back into the water and a new reflected wave $p_{c2}(x, t)$ is generated in the positive x direction in the core (Fig. 2). It can be shown that pressures at the front laminate due to these two waves, and the additional velocity generated in the laminate, v_2, are given by

$$p_{r2}(t) = -\rho c v_2(t) = E_1 e^{-\alpha t''} + \left(E_2 + E_3 t''\right) e^{-\beta t''} + E_4 e^{-\gamma t''} \tag{19}$$

and

$$p_{c2}(t) = F_1 e^{-\alpha t''} + \left(F_2 + F_3 t''\right) e^{-\beta t''} + F_4 e^{-\gamma t''}, \tag{20}$$

where

$$E_1 = \frac{2(\beta - \gamma) D_1}{\beta - \alpha}; \quad E_4 = 2D_3; \quad E_2 = -(E_1 + E_4); \quad E_3 = 2(\beta - \gamma) D_2 \tag{21}$$

$$F_1 = D_1 \left(1 - \frac{2\gamma}{\beta - \alpha}\right); \quad F_4 = D_3 \left(1 - \frac{2\gamma}{\beta - \gamma}\right); \quad F_2 = -(F_1 + F_4); \quad F_3 = -2\gamma D_2 \tag{22}$$

and

$$t'' = t' - \tau = t - 2\tau \tag{23}$$

After a further interval τ, $p_{c2}(x, t)$ reaches the rear laminate and generates a new reflected wave $p_{cr2}(x, t)$ in the core and an additional velocity w_2 in the laminate. The process repeats itself indefinitely, the pressure waves and additional velocity components having progressively smaller amplitudes. The resultant pressure and velocity histories at a given location can be found by superimposing the separate waves or velocity components.

3.3.2 Resultant Pressure Distributions and Histories

The resulting pressure histories in the water at various distances from the panel have been calculated for a number of explosion cases and typical sandwich layups using a spreadsheet program. The program also allows study of the through-the-thickness stresses and strains in the core and the motions of the skin laminates. The case of a

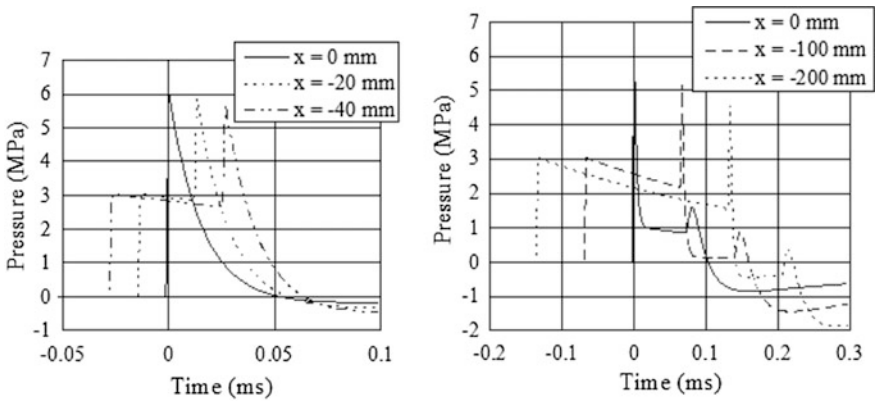

Fig. 3 Pressure histories in water at various distances from panel surface: thin plate (left) and sandwich plate (right). From Hayman [20]

thin plate or single-skin laminate can be analysed using the same program. Only the waves shown in Fig. 2 are included. Thus, the program does not give valid results for times when $p_{cr2}(x, t)$ or subsequently generated waves have reached the point in question. This means that, at the panel surface, $x = 0$, the results are only valid for $t \leq 4\tau$.

Figure 3 (left) shows the pressure histories at positions 0–40 mm from a thin plate having mass 24 kg/m^2 that is exposed to a shock wave with $p_0 = 3.0$ MPa and $\alpha = 2580$ s^{-1}. This shows that negative pressures are first generated at the plate surface, 0.05 ms after the shock wave arrives at the plate. Thus, if the cavitation tension is zero, cavitation can be expected at the plate surface. If a cavitation tension of 1 bar (0.1 MPa) is assumed, cavitation starts about 10 mm away from the panel.

Figure 3 (right) shows the corresponding case with a sandwich panel having approximately the same *total* mass per unit area. This panel has 4 mm thick GFRP skins and a 60 mm thick core of 200 kg/m^3 PVC foam. The analysis shows that, for zero cavitation tension, cavitation first occurs at the panel surface, about 0.10 ms after the shock wave arrives at the panel. The delay as compared to the thin plate is due to the time taken for the transmitted wave in the core to reach the rear skin and be reflected back to the panel/water interface ($2\tau \approx 0.07$ ms for this panel). However, at about the same time, cavitation also occurs independently at 125 mm from the panel as the negative part of the first reflected wave cancels the 'tail' of the incoming shock wave.

The influence of a nonzero cavitation tension can be studied from Fig. 3 (right) and the associated analysis. For a cavitation tension of 1 bar (0.1 MPa), there is little change. Cavitation is still initiated at the panel surface, at a time that is only a few microseconds later than for zero cavitation tension. The second cavitation site is moved about 15 mm further away from the panel, with initiation occurring at $t \approx 0.11$ ms, i.e. about 0.01 ms later than with zero cavitation tension.

Similar analyses with different shock waves show some interesting features. Increasing p_0 without changing α simply scales all the pressure histories up in proportion with p_0. This has no effect on the prediction of cavitation for the case of zero cavitation tension. However, it reduces the influence of a given nonzero cavitation tension. Reducing α (larger charges and/or standoffs) increases the distance between the second cavitation site and the panel, and delays cavitation initiation at this position. Increasing α (smaller charges and/or standoffs) leads to smaller cavitation distances, and can result in cavitation being initiated at the more remote position before it is initiated at the panel surface. For typical explosion cases considered in design of MCMV hulls, and typical sandwich layups for this application, the distance of the second cavitation site from the panel appears to be in the range 100–300 mm, in agreement with the observation mentioned in Sect. 3.2.

3.3.3 Subsequent Behaviour of Cavitated Region

Bleich and Sandler [4] considered the behaviour of a region of water between a submerged explosive charge and a thin plate suspended horizontally above it at the water surface. They showed that cavitation was first initiated just below the plate, and subsequently expanded and contracted with the upper and lower boundaries of the cavitated region migrating in a complex fashion, before the cavitated region finally closed. For the case of the vertical sandwich panel with cavitation occurring at two sites, the behaviour may be more complicated still. For this case, it was considered desirable to establish whether the mass of water between the two cavitation sites remains constant, and how long it remains detached from the panel and the main body of water.

By considering particle velocities associated with the respective pressure waves, it is possible to argue that the main body of water (outside the cavitated region) is moving towards the panel and slowing down. The water between the two cavitation sites has a zero resultant force acting on it as the pressures in the two cavitated regions can be assumed equal. This mass of water must therefore continue moving with a constant mean velocity once cavitation is established at the two locations, so the gap between this and the main body of water must continue to increase. Initially, the central region of the panel, which is uncoupled from the water, moves with constant velocity but then the boundary restraints cause the panel to slow down. The uncoupled water then catches up with the panel and the cavitated region adjacent to the panel closes. The panel and the water mass are now moving together, but are still separated from the main body of water.

The panel continues to slow down. Eventually, it reaches its maximum deflection and begins to swing back again towards its original position. Sooner or later, the main body of water and the panel will come to the same position. Observations in the DNV shock tests suggested that final cavitation closure occurred after the maximum deflection and stresses had been reached in the panel. (Later assessments are discussed in Sect. 4.3).

3.3.4 Formulae for Cavitation Initiation Time and Location

Cavitation at the panel surface will occur at time t_{cav1}, which is shortly after the reflected wave from the rear skin reaches the panel/water interface. This occurs at a time interval 2τ after arrival of the incoming shock wave, so

$$t_{\mathrm{cav1}} = 2\tau = 2h_c/c' \tag{24}$$

Cavitation at the second site occurs when the combined pressure from the incoming shock wave and the first reflected wave drop to a critical value p_{cav}, i.e. when

$$p_0 e^{-\alpha(t-x/c)} + B_1 e^{-\alpha(t+x/c)} + B_2 e^{-\beta(t+x/c)} = p_{\mathrm{cav}} \tag{25}$$

The location of the second cavitation site and the time at which cavitation is initiated there are found by calculating the smallest value of t that satisfies Eq. 25, and finding the corresponding value of x. This is achieved by differentiating Eq. 25 with respect to time, setting $dt/dx = 0$, and solving the resulting equation simultaneously with Eq. 25 itself. When $p_{\mathrm{cav}} \neq 0$, this requires numerical solution. However, when $p_{\mathrm{cav}} = 0$ explicit solutions exist for the position x_{cav2} (or distance ahead of the panel, $X_{\mathrm{cav2}} = -x_{\mathrm{cav2}}$) and the time t_{cav2} at which cavitation occurs

$$t_{\mathrm{cav2}} = \frac{1}{\beta-\alpha}\left[\frac{\alpha+\beta}{2\alpha}\ln\left(\frac{\alpha+\beta}{\alpha+\beta-2\gamma}\right) + \ln\left(\frac{\beta-\gamma}{\alpha}\right)\right] \tag{26}$$

and

$$X_{\mathrm{cav2}} = -x_{\mathrm{cav2}} = \frac{c}{2\alpha}\ln\left(\frac{\alpha+\beta}{\alpha+\beta-2\gamma}\right) \tag{27}$$

3.3.5 Formulae for Impulse and Kick-off Velocity

The kick-off velocity V_0 of the panel can be obtained by calculating first the impulse imparted to a unit area of the panel and water that moves with it, and then dividing by the combined mass per unit area M. The impulse J is calculated by integrating the pressure at the cavitation position with respect to time, from the instant the incoming shock wave arrives there to the time t_{cav2}. The main contribution J_i is from the incoming shock wave, but there is also a small, negative contribution J_{r1} from the first reflected wave

$$J = J_i + J_{r1}, \tag{28}$$

where

$$J_i = \frac{p_0}{\alpha}\left(1 - e^{-\alpha(t_{\text{cav2}} - x_{\text{cav2}}/c)}\right) \tag{29}$$

and

$$J_{r1} = p_0\left[\frac{2(\beta-\gamma)}{\beta(\beta-\alpha)}\left(1 - e^{-\beta(t_{\text{cav2}} + x_{\text{cav2}}/c)}\right) - \frac{\alpha + (\beta - 2\gamma)}{\alpha(\beta-\alpha)}\left(1 - e^{-\alpha(t_{\text{cav2}} + x_{\text{cav2}}/c)}\right)\right] \tag{30}$$

The kick-off velocity is then

$$V_0 = J/M, \tag{31}$$

where

$$M = 2m_f + \rho^{'} h_c + \rho X_{\text{cav2}} \tag{32}$$

3.3.6 Simplified Expressions

Some approximations can be made that simplify some of the above expressions. In practice $\beta \gg \alpha$, so that Eqs. 26 and 27 give

$$t_{\text{cav2}} \approx \frac{1}{2\alpha}\ln\left(\frac{\beta}{\beta - 2\gamma}\right) + \frac{1}{\beta}\ln\left(\frac{\beta-\gamma}{\alpha}\right) \tag{33}$$

and

$$X_{\text{cav2}} = -x_{\text{cav2}} \approx \frac{c}{2\alpha}\ln\left(\frac{\beta}{\beta - 2\gamma}\right) \tag{34}$$

A more approximate estimate of t_{cav2} is obtained by neglecting the second term on the right-hand side of Eq. 33. This is equivalent to taking

$$t_{\text{cav2}} \approx -x_{\text{cav2}}/c \tag{35}$$

In calculating the impulse, a good approximation is to neglect J_{r1} while using the simple relationship for t_{cav2}, Eq. 35, in Eq. 28:

$$J \approx J_i \approx \frac{P_0}{\alpha}\left(1 - e^{2\alpha x_{\text{cav2}}/c}\right) \tag{36}$$

3.3.7 Subsequent Global Panel Response

If it is assumed that the mass of water moving with the panel remains constant following cavitation initiation at the remoter cavitation site, analytical or numerical methods can be used, together with the above equations to estimate the subsequent response of the panel. Rough estimates can be obtained using the following formulae, which consider bending deformations but neglect both out-of-plane shear deformations and local bending of the individual skin laminates.

The period of oscillation, T, the maximum deflection, $\Delta_{\max}$ and the maximum laminate strain at the centre of the panel, $\varepsilon_{\max}$ can thus be estimated from

$$T = K_T \sqrt{\frac{M a^4}{E_f h_f \left(h_c + h_f\right)^2}}; \tag{37}$$

$$\Delta_{\max} = K_\Delta V_0 \sqrt{\frac{M a^4}{E_f h_f \left(h_c + h_f\right)^2}}; \tag{38}$$

$$\varepsilon_{\max} = K_\varepsilon V_0 \sqrt{\frac{M}{E_f h_f}} \tag{39}$$

In the above, the coefficients K_T, K_Δ and K_ε are functions of the plate aspect ratio and boundary support conditions and of Poisson's ratio for the skin laminates, and a is one of the panel dimensions.

3.3.8 Comparisons with Test Results and Other Analysis Methods

Figure 4 shows histories of compressive strain in the core of a sandwich panel resulting from (a) use of the above theory, without the simplifying approximations, (b) use of a one-dimensional finite element model consisting of 13 bar elements connected end-to-end and (c) measurements using a strain gauge embedded in the sandwich core. In case (b), the front laminate is modelled with four elements, the core with eight elements and the rear laminate by a single element. The applied shock load is simulated using Eq. (4): the free field pressure is doubled and a damper element used to give the velocity term.

The principal difference between curves (a) and (b) is the initial part of the response associated with the transmission of the shock wave through the front laminate, model (b) taking account of the finite thickness of this laminate. Also, case (a) is not valid after a time of about 0.12 ms, when the second reflection from the air side laminate reaches the point in question. Nevertheless, case (a) models the important aspects quite well.

The measured strain history (c) is very similar to curve (b). The differences may be partly due to the fact that the properties of the core were not measured accurately

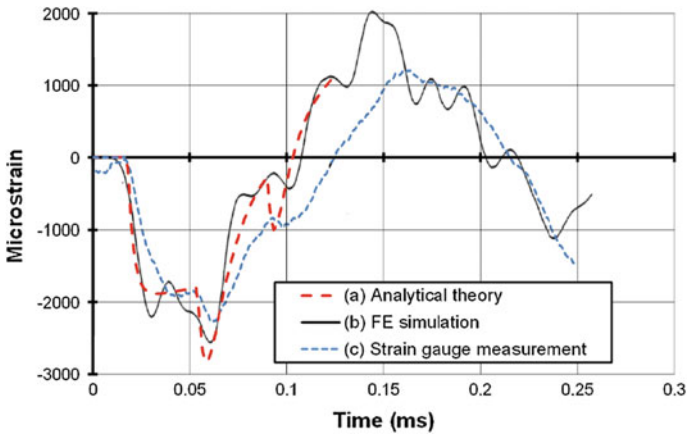

Fig. 4 Strain histories in the core by theory and experiment

at the relevant strain rates. There may also be some error in the measurement due to stiffening of the core by the strain gauges, though calibration tests suggested that this error is unlikely to be more than a few percent for the type of foam core and strain gauge used. Also, the position of the strain gauge does not correspond exactly to the Gauss point at which the FE analysis results are taken, and damping of the waves by the core is not taken into account in the models.

A further indication of the validity of the analytical model was obtained by studying how well Eqs. 37 and 39 agreed with experimental data from the UNDEX tests described in Sect. 3.1. The coefficients in the equations were obtained from thin plate solutions given in data books. Thus, the periods of oscillation estimated from strain gauge readings on four sandwich panels with the same overall dimensions but different layups, and with a wide range of shock loads, were plotted against values from Eq. 37, and maximum measured strains from the same tests were compared with those given by Eq. 39. The resulting plots are not included here as they contain a considerable degree of uncertainty, especially in relation to the assumed panel boundary conditions. Nonetheless, the trends predicted by the analyses were confirmed.

3.3.9 Effect of Sandwich Layup

The simple model described above allows rapid evaluation of the influence of such aspects as sandwich layup on underwater explosion response.

Influence of core density For typical PVC foam cores, increasing the density leads to a corresponding increase in elastic modulus, so that the acoustic speed is scarcely affected. However, the increased density itself results in reflected and transmitted waves of higher amplitude. This leads to higher through-thickness stresses in the

core, and slightly higher pressures in the water. There is a marked increase in the distance X_{cav2} of the more remote cavitation site from the panel. For the same incoming shock wave, this distance is roughly proportional to the core density. The impulse applied to the panel and water layer is also increased, so that the panel deflection and laminate stresses are increased somewhat.

Influence of core thickness Changing the core thickness has no effect on cavitation at the more remote site but has a major influence on the time at which cavitation occurs at the panel surface. For a very thick core, cavitation at the more remote site is likely to occur first. For very thin cores, the situation approaches that of a thin plate, and cavitation may occur so early at the plate surface that the reflected wave is prevented from generating cavitation at a more remote position. Provided the behaviour does not change fundamentally, the main visible effect of an increase in core thickness predicted by the present theory is a reduction in panel deflection, but the maximum stress in the laminates is scarcely affected.

Influence of laminate thickness Increasing or decreasing the mass per unit area of the skin laminates has a similar effect to increasing or decreasing the core thickness, except that the laminate stresses are reduced proportionately with the maximum deflection.

3.3.10 Comments and Conclusions from the Study

Simple wave theory was used to derive cavitation conditions, and hence to estimate the kick-off velocity of a sandwich panel when subjected to underwater shock loadings, together with the mass of water that moves with the panel. The theory appeared to explain several observations from explosion tests:

- It showed why a layer of water with thickness of order 20 cm moves with the panel.
- It demonstrated that the thickness of this layer, and hence the period of oscillation, varies with the applied shock load.
- It explained the observed variation of both period and maximum laminate strain with panel layup and shock load.

In the original paper, it was noted that, in principle, it would be quite straight forward to include waves generated by further encounters with the skin laminates. However, the analytical expressions become more complex. This is only needed if prediction of pressures, stresses, etc., are needed for later times. The analytical theory presented works best for sandwich panels with thin skin laminates. For thicker skins, it may be necessary to correct the results for the time delays as the stresses due to the respective waves build up in the skin laminates.

In many practical applications involving hulls of surface ships, the incoming primary shock wave is truncated by the arrival of a tensile reflected wave from the free water surface. This effect is easily included in the analytical model.

The major question that was left open concerned the possible movement of cavitation boundaries following initial cavitation at the two sites as described previously. To provide insight into this point, it was suggested that analyses of the type performed by Bleich and Sandler [4] or Driels [14] would need to be performed for some typical cases. In fact, Mäkinen and others have taken up this point, as discussed in Sect. 4.

4 Subsequent Simulation Studies

Several studies of the response of sandwich panels to UNDEX loading have been published since 1995. Some follow directly on from Hayman [20], by considering primarily elastic response of hull panels with polymer foam cores. Others are more concerned with providing strength and energy absorption as a protection against UNDEX shock, and consider a wider range of materials (in particular utilising the ductility of metals). The following summarises studies of both types, with focus on the modelling of FSI effects and associated cavitation.

4.1 Studies by Mäkinen and Colleagues

At the same conference as that at which the work summarised in Sect. 3.3 was presented, Mäkinen [27] also presented the results of some tests and simulations on a foam-cored GFRP sandwich panel. The simulation was carried out using the DAA method as implemented in the USA-STAGS software. The surface cut-off effect was included, as was cavitation at the panel surface, but the possibility of cavitation at other locations does not seem to have been considered. The author commented that because of surface cut-off effects the important parts of the response all occurred at early times, so that the use of simpler methods, such as that described by Moyer et al. [34], referred to in Sect. 3.2, could be expected to give good results.

Mäkinen followed up the above work in a doctoral thesis [29] that included two published journal articles, one conference paper and one paper that does not appear to have been published outside the thesis. First, he investigated [28] the formulation of relevant cavitation models and compared their predictions. Second [30], he applied an appropriate model to the incidence of a primary shock wave on a 1-D model for the through-thickness response of a foam-cored sandwich panel, taking account of movement of the cavitation boundaries. Thus, Hayman's analysis was modified and extended to include movement of the cavitation boundaries and also to include further internal reflections of the shock wave inside the sandwich core. This treatment was still entirely one-dimensional. It gave predictions very similar to

Hayman's in terms of stress and strain values inside the core. A further paper by Mäkinen and Kadyrov [31] applied this one-dimensional fluid–structure interaction model (with cavitation) to simulate an experimental test carried out in the Swedish MCMV programme. The test arrangement was that described by Moyer et al. [34]. Rather few details are provided from the tests, but the agreement between modelling and testing appears to have been very satisfactory. Unfortunately, it is not possible to compare the analysis directly with Hayman's simpler model. Note that this modelling is still essentially considering an early time approximation since it is an acoustic model and fluid flows across the plate are not considered. Mäkinen's thesis includes a further paper that does not appear to have been published; this applies the same approach in a parametric study of sandwich beams (as opposed to panels) with differing layups.

4.2 Studies Concerned with Protection and Energy Absorption

In the late 1990s, interest was aroused in the potential of sandwich structures to absorb energy in collisions and under blast loadings. The main objective was to establish the extent to which sandwich beams or panels would perform better than solid beams or plates of the same mass. Some of the studies performed were funded by the US Office of Naval Research (ONR). They were primarily concerned with metal sandwich structures, including some with (mainly metal) foam cores, and considered nonlinear, inelastic behaviour. They are briefly described here because they show how the FSI and cavitation modelling has been developed since Hayman's and Mäkinen's studies.

Deshpande and Fleck [8] presented constitutive laws for metal (aluminium alloy) foams that might in future be used in sandwich cores. The same authors subsequently [9] investigated the multiaxial yield behaviour of some PVC foams.

Xue and Hutchinson [45] appear to be among the first to consider specifically blast loading on metal sandwich structures. They considered a metal sandwich, with properties appropriate to truss cores, and focused on achieving high strength and energy absorption. They neglected strain rate dependence and FSI, while referring briefly to Mäkinen [29, 30], but mentioned that these simplifications could be expected to lead to pessimistic results in the case of UNDEX loadings. The same authors [46] later published a comparative study of blast-resistant metal sandwich plates.

Deshpande and Fleck [10] considered both metal and PVC foam-cored sandwich beams under air blast loading. They considered two phases—core compression (treated as inelastic) and global beam bending and stretching. They suggested that the results could be applied to UNDEX loadings but mentioned that FSI would have a beneficial effect. Fleck and Deshpande [15] compared a series of competing metallic core concepts. They divided the response into three stages: Stage I,

fluid–structure interaction (the initial primary shock transient, during which they assumed that the core and back face would remain stationary); Stage II, core crushing; and Stage III, overall bending and stretching. Stages I and II were treated one dimensionally, as in Hayman [20], Mäkinen and Kadyrov [31] and Mäkinen [30]. For UNDEX cases, they also introduced an 'FSI parameter', $\psi = \rho c/\alpha m_f$ (using the notation of Sect. 3.2), by which the theoretical impulse transmitted to a fixed, rigid structure would be reduced by the motion of the skin laminate. The sandwich cores they considered were relatively thick (0.1–1.0 m).

Hutchinson and Xue [24] studied the optimisation of metal sandwich plates for resistance to short pressure pulses. They followed the approach of Fleck and Deshpande [15], but improved on the FSI description of Stage I by accounting for the resistance the core offers to the motion of the front face sheet. They note that this results in cavitation being initiated some way from the plate surface, rather than at the plate surface itself. They then assume that the layer of water between the plate and the cavitation plane moves with the plate and remains with constant thickness —just as assumed by Hayman [20]. They note that the cavitated region will in fact close after some time, causing an additional transmitted impulse, but argue that this is small compared to the main impulse. Liang et al. [26] made further refinements to the model of Hutchinson and Xue [24], to give a better estimate of the momentum transmitted to the panel from the water taking account of the motion of the cavitation boundaries. Deshpande and Fleck [11] also used one-dimensional models to explore the FSI effects, including cavitation, for metal sandwich panels with crushable foam cores. They developed extensive maps showing differing regimes of behaviour. They treated the cores as inelastic, and observed that in practical cases of interest the core can be treated as an ideally plastic-locking solid (i.e. as rigid-plastic with a densification limit). It should be noted that the explosion cases they considered as typical have appreciably shorter pulse durations (around 0.1 ms) than in the Norwegian and Swedish studies.

Schiffer [39], in a recent doctoral thesis, investigated the response of both water- and air-backed composite laminates using both 1-D models (with FSI and modelling of moving cavitation boundaries) and corresponding tests using a shock tube. Based on a part of this work, Schiffer and Tagarielli [40] considered the specific case of a foam-cored sandwich layup with metal face sheets. FSI experiments and FE calculations were performed in order to examine the one-dimensional response of both water-backed and air-backed sandwich plates subject to blast loading in either deep or shallow water. The sandwich plates had rigid face sheets and low-density metal and polymer foam cores. The experiments were conducted in a transparent shock tube, allowing measurements of both structural responses and cavitation processes in the fluid. The simulations focused on estimation of the position of cavitation initiation, movement of the cavitation fronts, and the transmitted impulse and its dependence on parameters such as the core strength and stiffness and water pressure. It represented a further refinement of the approach of Liang et al. [26]. The study was more nuanced than previous ones, and showed that the sandwich solutions did not always perform better than corresponding solid plates.

4.3 Recent Work

Extensive studies, supported by the ONR, have been carried out in recent years at Imperial College London (ICL) into the underwater and air blast performance of polymer foam-cored sandwich panels. The work has largely involved physical testing [3, 7], and modelling has mainly been confined to air blast cases. The UNDEX testing has been confined to quite small panels (0.4 m × 0.3 m) exposed to blasts from small charges (1.0–1.4 kg of C4 explosive) at small standoffs generating peak pressures (30–43 MPa) that are far higher than in the Norwegian tests reported in Sect. 3.1. The resulting response involved severe compression of the SAN foam cores combined with face sheet damage.

In a recent collaboration between the present author and researchers from ICL and Nanyang Technological University, Singapore, attempts have been made to simulate some of the UNDEX tests reported in Sect. 3.1 using the explosion modeller and acoustic elements in ABAQUS. The initial trials are described below. Further trials have been conducted but are not reported here. The purpose of the studies has been to establish whether the proposed modelling approach can reproduce the main features of the response of foam-cored sandwich panels to a primary shock wave. The approach is confined to 'early times', in the sense that fluid flow effects are not included; however, use of a three-dimensional model removes some of the restrictions imposed by one-dimensional modelling of the acoustic phase in earlier analyses. Inclusion of the test box in the model reduced the uncertainties regarding panel boundary conditions.

4.3.1 Test Case Considered

Data from the two similar tests in Series 1 (Sect. 3.1) were used to validate the model results. Each face sheet laminate consisted of one layer of 300 g/m^2 chopped strand mat (CSM), two layers of 800 g/m^2 woven roving (WR) fibres each with an additional 300 g/m^2 CSM and a final 300 g/m^2 CSM layer. The matrix was iso-polyester Norpol 72–80, and the fibre weight fraction was approximately 50%. The total thickness of each face sheet was approximately 3.5 mm. A 60 mm thick Divinycell H200 closed cell PVC foam core was used, giving a total panel thickness of 67 mm. The blast pressures were generated with 14 kg of TNT at 30 m standoff distance. This relatively low blast level was chosen in order to validate the modelling method without the need for implementing accurate material failure and degradation laws.

4.3.2 FEA Models

The FEA models were built using ABAQUS 6.9 (Dassault Systèmes [6]). Initially, the test panel was modelled in isolation, assuming clamped boundary conditions.

While this was seen to give promising results, it was found that improved agreement between tests and simulation could be achieved by including the steel test box in the model. A quarter model of the panel and test box with appropriate symmetry boundary conditions was used (Fig. 5), though this does not allow accurate modelling of the variation of static pressure with depth. The core was modelled using 3D hexahedral stress elements with reduced integration and hourglass control. Quadrilateral shell elements with reduced integration and hourglass control were used for the skin laminates and for the steel box components. An element size of 10 mm was used throughout.

The water surrounding the test box and panel was modelled separately using tetrahedral acoustic elements. These elements have a pressure degree of freedom and are therefore able to model the blast wave propagation. Additionally, cavitation can be simulated by setting a minimum pressure the medium can sustain. The degree of FSI that is modelled corresponds to the 'early time' solution for a thin plate presented by Taylor [42]; it does not include fluid flow effects.

The parameters for the material models were obtained from tests performed on the same material types used in the panel manufacture. For simplicity, the H200 foam core was modelled with an isotropic, linear elastic material. The assumed Young's modulus was 250 MPa and the Poisson's ratio was 0.39. Each face laminate was modelled as a single layer shell. A laminar anisotropic elastic model was used, so that appropriate damage models could be used in later analyses. However, the same overall properties were applied in both directions. The Young's modulus and the shear modulus were assumed to be 14.6 GPa and 2.8 GPa, respectively, whilst the Poisson's ratio used was 0.17. The steel box was modelled with a linear elastic material with density 7800 kg/m^3, Young's modulus 210 GPa and Poisson's ratio 0.3. The density of the sea water was assumed to be 1025 kg/m^3 and the bulk modulus to be 2.1 GPa, whilst the cavitation limit was set at −75 kPa (tension, absolute pressure). Note that, because of the static ambient pressure of approximately 150 kPa due to atmospheric pressure and the 5 m water depth, this

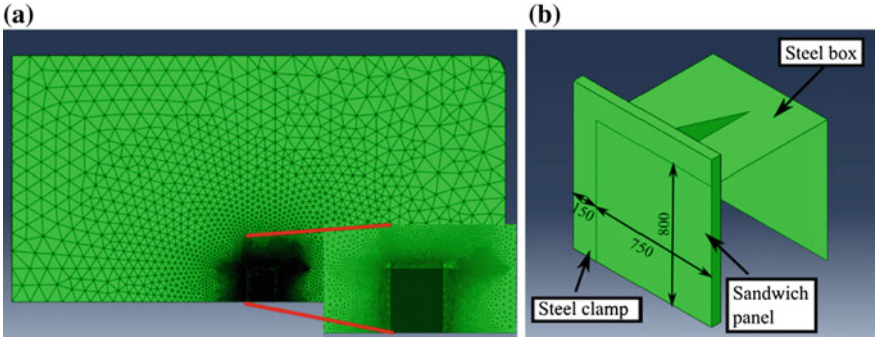

Fig. 5 Images of the FEA quarter model showing: **a** the acoustic mesh around the box structure, and **b** the test panel and the steel box providing the key dimensions of the panel

requires the shock wave to induce a pressure of −225 kPa in order to initiate cavitation.

The inbuilt underwater blast simulation tool in ABAQUS was employed to simulate the blast pressure waves. The tool uses equations derived by Geers and Hunter [17] to simulate both the initial shock wave and the dynamics of the gas bubble created at the charge location. In this case, the bubble pulses were neglected due to the large charge distance, and the analysis was confined to the effects of the initial shock wave. The software required the input of similitude parameters for the explosive used as well as the physical characteristics of the blast, including its position and the quantity of explosive material. The relevant parameters were obtained from Geers and Hunter [17], based on 1.52 g/cm^3 TNT.

4.3.3 Results

The results from the FE models were compared to the strain and pressure histories recorded during the blast tests. The FE pressure results were extracted at a location close to that of the pressure gauge. The maximum simulated pressure was 2.75 MPa, compared to recorded values of 3.0 MPa in both tests. Whilst the simulated peak is lower than the measured data by approximately 10%, the FE pressure rise time was longer, with a smoother rise and peak. The impulse recorded in the experimental tests was approximately 800 Pa s in the first millisecond, shortly after which the reflected wave from the target reached the sensor and the recorded signals became chaotic. The FE impulse in the same time period was 1050 Pa s. Note that this is the integral of the incoming pressure at the gauge with respect to time, and is not the same as the impulse actually imparted to the panel.

The strains at the centre of the panel on the water side and on the air side were compared, as shown in Figs. 6 and 7. The FE results for the water side strains matched closely the experimental data until about 15 ms. The air side data matched the experimental results up to the first peak at about 6 ms. Following this, the results diverge, with the strains decreasing less rapidly in the numerical analysis data.

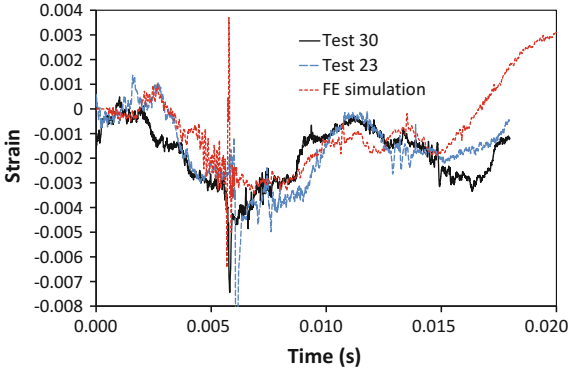

Fig. 6 Water side vertical strains. The FEA results are compared to two sets of experimental data

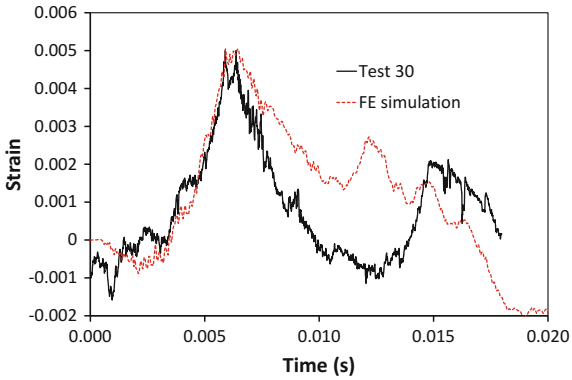

Fig. 7 Air side vertical strains. The FEA results are compared to the test results

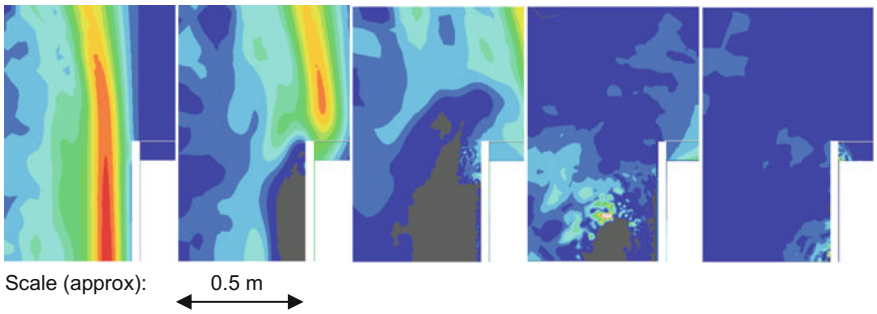

Fig. 8 Simulated pressure fields at time instants $t = 0$, 0.25, 0.5, 2.5 and 5.5 ms from arrival of incident shock wave at panel surface. Cavitated regions are shown in grey

The pressure fields at successive time instants have also been studied (Fig. 8). Immediately after arrival of the shock wave at the panel surface, the simulation indicates a region of cavitation adjacent to the front skin laminate. However, after less than 0.25 ms, a layer of uncavitated water appears at the panel surface, with a region of cavitation beyond this. The thickness of this uncavitated water layer grows rapidly to about 150 mm over the next millisecond or so. Then a cavitation layer reappears at the panel surface, while the thickness of the region of uncavitated water increases to a maximum between 200 and 250 mm while its boundary becomes more irregular. The picture becomes more chaotic, until eventually the last region of cavitation collapses, at about 5 ms after arrival of the shock wave. This probably explains the sharp spike in the strain histories (both measured and simulated) seen in Fig. 6. Thus, over a significant part of the response there appears to have been an uncavitated layer of water adjacent to the panel surface, as predicted by the simplified theory of Hayman [20]. However, whereas Hayman's early theory predicts an uncavitated layer with thickness approximately 150 mm for the present

case, and assumes this to remain constant, the FE simulation shows that it varies with time, reaching a maximum value somewhat greater than this magnitude before the picture becomes chaotic and the cavitation begins to close again.

4.3.4 Discussion and Conclusions

The FE analysis showed that many of the important features of the measured response could be replicated using the UNDEX simulation option in ABAQUS, combined with the use of acoustic elements for the water. The measured strain histories at the centre of the wet face laminate were well reproduced to times well beyond the peak deformation. That at the centre of the air side laminate was also accurately reproduced up to a time just after the peak response, but then the simulation gave a less rapid fall in strain values than the measurements. The UNDEX simulation option of ABAQUS approximately replicated the peak of the generated pressure pulse, though the numerical result was somewhat lower than the measured value, and the rise time was longer, which affected the impulse and the pulse shape. This may have changed the conditions regulating the cavitation of the medium. Whilst this introduces some inaccuracy in the model, the strain results obtained indicate that the system might be relatively insensitive to this in the simulation. The results suggest that the 'early time' acoustic model with cavitation is able to predict the maximum panel deformations and stresses, but effects due to the fluid flows around the target need to be taken into account, using a full computational fluid mechanics model, if the response at later times is to be investigated.

The simulation showed the formation and eventual closure of a region of cavitation ahead of the target panel, while for the major part of the response up to the peak deformation, an uncavitated layer of water moves with the panel. This is consistent with the predictions by Hayman [20] using simple one-dimensional plane wave propagation theory. However, while Hayman assumed that the thickness of the uncavitated layer would remain constant, the present simulation shows that the cavitation boundaries move and the thickness varies with time.

Some differences between the predicted and measured responses may be due to inaccuracies in the model of the box, which had to be simplified in the simulation. Additionally, the air medium inside the box was not included in this model.

5 Conclusions and Implications for Shock Mitigation Studies

An attempt has been made to trace the history of naval (and some relevant civilian) vessels using foam-cored sandwich, with particular focus on those with UNDEX requirements, and on the associated testing and modelling. The early modelling work performed by the author around 1990 has been summarised, as have the

developments of this by Mäkinen, and the work performed by Hutchinson and colleagues at Harvard and by Fleck, Deshpande and others at Cambridge, which focused especially on metallic sandwich with inelastic cores but included progressively improved FSI and cavitation descriptions. It culminates with quite recent work at the University of Oxford and Imperial College London, the latter in collaboration with the author.

Several points have arisen that have implications for shock mitigation studies:

- There are significant differences between modelling requirements for MCMV hull design and those for blast protection, and the results and conclusions cannot necessarily be transferred between these types of applications. Hull design for MCMVs focuses on avoidance of damage and maintenance of predominantly elastic behaviour, while blast protection focuses on use of inelastic behaviour to absorb energy.
- Sandwich panel responses for both types of application deviate from the classical theory by Taylor for thin plates, but in different ways.
- Changing the sandwich layup may be used to reduce the transferred impulse, but may at the same time reduce the resistance to global deformations.
- Trends observed for air blast cannot usually be transferred to water blast.
- Failure mechanisms for sandwich panels with UNDEX loading include.
  - Excessive crushing and damage to the core, possibly resulting in reduction or elimination of tensile through-thickness strength.
  - Failure under global panel deformation, due to either laminate tension/compression or core shear failure.

Changing the UNDEX shock case (e.g. between small charges at small standoffs and large charges at large standoffs), the panel size and support conditions, or the test or model configuration, may change the critical mechanism. Thus, it is important to ensure that shock mitigation studies reproduce conditions as close as possible to the envisaged application.

Acknowledgements Thanks are due to the Norwegian Defence Logistics Organisation/Naval Systems for permission to use the UNDEX measurement data. The work at Imperial College London (ICL) is led by Prof. John Dear, and at the time was supported by ONR Grant no. N00014-12-1-0403 as part of the Solid Mechanics Program (SMP) under Program Manager Dr. Yapa D.S. Rajapakse. Dr. Hayman's work is also supported by the SMP/Dr. Rajapakse. This support is gratefully acknowledged. The FE modelling presented in Sect. 4.3 was performed by the Dr. Paolo Del Linz (formerly of ICL) at Nanyang Technological University, Singapore. Advice on the FE modelling was provided by Dr. Hari Arora of the Department of Bioengineering, ICL. These contributions are also gratefully acknowledged.

References

1. Anon. (1985). Navy awards Bell Aerospace Textron $27.3-million contract for new minesweeper hunter. *Maritime Reporter & Engineering News 47*(2), 28–29.

2. Anon. (2011). MSH-1 *Cardinal* Minesweeper Hunter (MSH). http://www.globalsecurity.org/military/systems/ship/msh-1.htm.
3. Arora, H., Hooper, P. A., & Dear, J. P. (2012). The effects of air and underwater blast on composite sandwich panels and tubular laminate structures. *Experimental Mechanics, 52,* 59–81. https://doi.org/10.1007/s11340-011-9500-z.
4. Bleich, H. H., & Sandler, I. S. (1970). Interaction between structures and bilinear fluids. *International Journal of Solids and Structures, 6,* 617–639.
5. Chalmers, D. W., Osborn, R. J., & Bunny, A. (1984). Hull construction of MCMVs in the United Kingdom. In: Proceedings of International Symposium on Mine Warfare Vessels and Systems, 12–15 June 1984. London: Royal Institution of Naval Architects.
6. Dassault Systèmes Simulia Corp. (2009). Abaqus analysis manual v6.9. Providence, RI.
7. Dear, J. P., Rolfe, E., Kelly, M., Arora, H., & Hooper, P. A. (2017). Blast performance of composite sandwich structures. *Procedia Engineering, 173,* 471–478. https://doi.org/10.1016/j.proeng.2016.12.065.
8. Deshpande, V. S., & Fleck, N. A. (2000). Isotropic constitutive models for metallic foams. *Journal of the Mechanics and Physics of Solids, 48,* 1253–1283.
9. Deshpande, V. S., & Fleck, N. A. (2001). Multi-axial yield behaviour of polymer foams. *Acta Materialia, 49,* 1859–1866.
10. Deshpande, V. S., & Fleck, N. A. (2003). Blast resistance of sandwich beams. In *Proceedings of the 6th International Conference on Sandwich Construction*, *fort lauderdale* 31 March–2 April 2003.
11. Deshpande, V. S., & Fleck, N. A. (2005). One-dimensional response of sandwich plates to underwater shock loading. *Journal of the Mechanics and Physics of Solids 53*.
12. Dixon, R. H, Ramsey, B. W., & Usher, P. J. (1972). Design and build of the GRP hull of HMS *Wilton*. In *Symposium on GRP Ship Construction*, October 1972, London: Royal Institution of Naval Architects.
13. Dodkins, A. R. (1989). The structural design of the single role minehunter. In *Proceedings of Warship '89 International Symposium on Mine Warfare Vessels and Systems* 2, 8–10 May 1989. London: Royal Institution of Naval Architects.
14. Driels, M. R. (1980). The effect of a non-zero cavitation tension on the damage sustained by a target plate subject to an underwater explosion. *Journal of Sound and Vibration, 73*(4), 533–545.
15. Fleck, N. A., & Deshpande, V. S. (2004). The resistance of clamped sandwich beams to shock loading. *Journal of Applied Mechanics, 71,* 386–401.
16. Geers, T. L. (1978). Doubly asymptotic approximations for transient motions of submerged structures. *Journal of the Acoustic Society of America, 64*(5), 1500–1508.
17. Geers, T. L., & Hunter, K. S. (2002). An integrated wave-effects model for an underwater explosion bubble. *Journal of the Acoustical Society of America 111*, 1584–1601. https://doi.org/10.1121/1.1458590.
18. Gullberg, O., & Olsson, K.-A. (1990). Design and construction of GRP sandwich ship hulls. *Marine Structures, 3,* 93–109.
19. Hall, D. J., & Robson, B. L. (1984). A review of the design and materials evaluation programme for the GRP/foam sandwich composite hull of the RAN minehunter. *Composites, 15*(4), 266–276.
20. Hayman, B. (1995). Underwater explosion loading on foam-cored sandwich panels. In *Sandwich Construction 3*, *Proceedings of the 3rd International Conference on Sandwich Construction*, Southampton, 11–15 September 1995.
21. Hellbratt, S.-E, & Gullberg, O. (1988). The high speed passenger ferry *SES Jet Rider*. In *Proceedings of the 2nd International Conference on Marine Applications of Composite Materials*, Melbourne, Florida, USA, 21–23 March 1988.
22. Hellbratt, S.-E, & Gullberg, O. (1989). The development of the GRP-sandwich technique for large marine structures. In *Proceedings of the 1st International Conference on Sandwich Constructions*, Stockholm, 19–21 June 1989.

23. Henton, D. (1967). Glass reinforced plastics in the Royal Navy. *Transactions of the Royal Institution of Naval Architects, 109,* 487–501.
24. Hutchinson, J. W., & Xue, Z. (2005). Metal sandwich plates optimized for pressure impulses. *International Journal of Mechanical Sciences, 47,* 545–569.
25. Keil, A. H. (1961). *The response of ships to underwater explosions,* 16–17 November 1961. New York: Society of Naval Architects and Marine Engineers Annual Meeting.
26. Liang, Y., Spuskanyuk, A. V., Hayhurst, D. R., Hutchinson, J. W., McMeeking, R. M., & Evans, A. G. (2007). The response of metallic sandwich panels to water blast. *Journal of Applied Mechanics, 74,* 81–99.
27. Mäkinen, K.-E. (1995). Numerical and experimental results for shock loaded sandwich panels. In *Sandwich Construction 3*, *Proceedings of the 3rd International Conference on Sandwich Construction*, Southampton, 11–15 September 1995.
28. Mäkinen, K.-E. (1998). Cavitation models for structures excited by a plane shock wave. *Journal of Fluids and Structures, 12,* 85–101.
29. Mäkinen, K.-E. (1999). *Underwater shock loaded sandwich structures*. Doctoral Thesis, Report 99–01, Royal Institute of Technology Department of Aeronautics: Sweden.
30. Mäkinen, K.-E. (1999). The transverse response of sandwich panels to an underwater shock wave. *Journal of Fluids and Structures, 13*(5), 631–646. https://doi.org/10.1006/jfls.1999.0222.
31. Mäkinen, K.-E., & Kadyrov, S. (1998). A 1-D fluid sandwich interaction model for the early time underwater shock loading. In *Proceedings of the 4th International Conference on Sandwich Construction*, Stockholm, Sweden, 9–11 June 1998.
32. Mouritz, A. P., Gellert, E., Burchill, P., & Challis, K. (2001). Review of advanced composite structures for naval ships and submarines. *Composite Structures, 53,* 21–41.
33. Mouritz, A. P., Saunders, D. S., & Buckley, S. (1993). The damage and failure of GRP laminates by underwater explosion shock loading. In *5th Australian Aeronautical Conference,* Melbourne, 13–15 September 1993. The Institution of Engineers, Australia, National Conference Publication No. 93/6.
34. Moyer, E. T., Amir, G. G., Olsson, K. A., & Hellbratt, S. E. (1992). Response of GRP sandwich structures subject to shock loading. In *Proceedings of the 2nd International Conference on Sandwich Constructions*, Gainesville, USA, March 9–12 1992.
35. Olsson, K.-A., & Lönnö, A. (1992). Sandwich constructions—recent research and development: GRP-sandwich technology for high-speed marine vessels. In *Proceedings of the 2nd International Conference on Sandwich Constructions*, Gainesville, USA, 9–12 March 1992.
36. Robson, B. L. (1984). The RAN GRP minehunter—a status report. In *Proceedings of International Symposium on Mine Warfare Vessels and Systems*, 12–15 June 1984. London: Royal Institution of Naval Architects.
37. Robson, B. L. (1989). The Royal Australian Navy inshore minehunter—lessons learned. In *Proceedings of the 1st International Conference on Sandwich Construction*, Stockholm, 19–21 June 1989.
38. Royal Institution of Naval Architects. (1984). In *Proceedings*, *International Symposium on Mine Warfare Vessels and Systems* (3 Vols.). London: RINA.
39. Schiffer, A. (2013). *The response of submerged structures to underwater blast*. Thesis submitted for the degree of D.Phil in Engineering Science: University of Oxford, UK.
40. Schiffer, A., & Tagarielli, V. L. (2014). One-dimensional response of sandwich plates to underwater blast: Fluid-structure interaction experiments and simulations. *International Journal of Impact Engineering, 71,* 34–49.
41. Sjögren, J., Celsing, C.-G., Olsson, K.-A., Levander, C.-G., & Hellbrat, S.-E. (1984). Swedish development of MCMV-hull design and production. In *Proceedings of International Symposium on Mine Warfare Vessels and Systems*, 12–15 June 1984. London: Royal Institution of Naval Architects.
42. Taylor GI (1941). The pressure and impulse of submarine explosion waves on plates. In: Underwater explosion research: a compendium of British and American reports. US Office of

Naval Research, Washington, DC, USA, 1950. Also in Taylor, G. I. (1963) *The scientific papers of G. I. Taylor*, (Vol. III, pp. 287–303). Cambridge University Press: Cambridge, UK.
43. Trimming, M. (1984). Monocoque GRP minehunters. In *Proceedings of International Symposium on Mine Warfare Vessels and Systems*, 12–15 June 1984. London: Royal Institution of Naval Architects.
44. Trimming, M., Fantacci, G., & Buccianti, A. (1989). US Navy minehunter coastal (MHC) O*sprey* class. In *Proceedings of Warship '89 International Symposium on Mine Warfare Vessels and Systems*, 8–10 May 1989. London: Royal Institution of Naval Architects.
45. Xue, Z., & Hutchinson, J. W. (2003). Preliminary assessment of sandwich plates subject to blast loads. *International Journal of Mechanical Sciences, 45,* 687–705.
46. Xue, Z., & Hutchinson, J. W. (2004). A comparative study of impulse-resistant metal sandwich plates. *International Journal of Impact Engineering, 30,* 1283–1305.